Published by Institute of Physics Publishing for SISSA

Received: *November 30, 2007*
Revised: *January 16, 2008*
Accepted: *February 8, 2008*
Published: *February 18, 2008*

Two universal extra dimensions and spinless photons at the ILC

Ayres Freitas

University of Chicago, 5640 S. Ellis Ave.,
Chicago, IL 60637, U.S.A., and
HEP Division, Argonne National Laboratory,
9700 Cass Ave., Argonne, IL 60439, U.S.A.
E-mail: afreitas@hep.anl.gov

Kyoungchul Kong

Theoretical Physics Department, Fermilab,
Batavia, IL 60510, U.S.A.
E-mail: kckong@fnal.gov

Abstract: We study the ILC phenomenology of Kaluza-Klein (KK) modes along two universal extra dimensions compactified on the chiral square. We compute production cross sections of various (1,0) particles at the ILC with $\sqrt{s} = 1\,\text{TeV}$, focusing on decays of KK-leptons and the KK partner of the hypercharge gauge boson down to the "spinless photon", which is the lightest KK particle. We contrast this model to one universal extra dimension with KK-photon (spin-1) and supersymmetry with neutralino (spin-1/2) or gravitino (spin-3/2) dark matter. We also investigate the discovery potential for (1,1) KK bosons as s-channel resonances.

Keywords: Field Theories in Higher Dimensions, Beyond Standard Model.

JHEP02(2008)068

Contents

1. Introduction

Among many models for new physics beyond the standard model (SM), supersymmetry (SUSY) and models with extra dimensions play a special role, since they introduce a new symmetry which is felt by all particles. Therefore they lead to a multiplication of the particle content with respect to the SM. The new particles can be protected by a discrete symmetry, thus allowing for a natural stable dark matter candidate, which usually is partner of the SM gauge bosons. In the most widely known examples of the Minimal Supersymmetric standard model (MSSM) and the standard model with one universal extra dimension (5DSM) [1] the typical dark matter candidates are fermions (neutralino or gravitino) or Kaluza-Klein (KK) vector bosons, respectively.[1] In the standard model with two universal extra dimensions (6DSM) [2, 3], on the other hand, the lightest Kaluza-Klein particle (LKP) is expected to be a scalar, which is an adjoint under the gauge groups. It originates from the polarization modes of the KK vector bosons along the extra dimensions, which upon compactification receives a smaller mass than the usual four polarization modes of the KK vector boson.

The structure of the 6DSM and its phenomenology at hadron colliders has been studied in several articles [2 – 7]. Furthermore it was shown that the scalar adjoint could provide a good dark matter candidate [8 – 10]. Although there might be some tension between the

[1] It should be pointed out, however, that if the MSSM is extended by a right-handed sneutrino superfield, the right-chiral sneutrino could be a viable scalar dark matter candidate.

JHEP02(2008)068

region consistent with dark matter and the collider bounds from Tevatron, a light LKP (relatively large radius R of the extra dimensions) is preferred. As a consequence, this is an excellent opportunity for an e^+e^- linear collider like ILC with $\sqrt{s} = 1\,\text{TeV}$ to cover much of the particle spectrum.

If new particles are found that are compatible with supersymmetry or extra-dimensional models, the determination of the spin of the stable dark matter candidate will be crucial for understanding the experimental discoveries. Since this stable particle is weakly interacting and escapes the detector leaving a missing energy signal, it is very difficult to measure its spin at hadron colliders, especially if the particle spectrum is nearly degenerate (see refs. [11, 12] and references therein). However, with the advantage of a well-defined initial state with controllable center-of-mass energy and beam polarization, spin determination of new particles is possible without serious model assumptions.

In this paper, we study the phenomenology of KK-particles in the 6DSM at the ILC with $\sqrt{s} = 1\,\text{TeV}$. In particular we analyze how the nature of the LKP can be explored in the decay of other KK partners. Another interesting feature of the 6DSM is the existence of modes with even KK parity and a mass that is only larger by a factor of $\sqrt{2}$ with respect to the lowest KK modes — in contrast to the 5DSM, where the KK mode masses are separated by integer ratios. These particles can be produced singly at the ILC, so that they are quite likely to be within the energy reach of the collider.

We start by reviewing the standard model in two universal extra dimensions in section 2 and proceed in section 3 to calculate production cross sections of various (1,0) particles at an e^+e^- linear collider with $\sqrt{s} = 1\,\text{TeV}$. We also discuss how those produced particles decay, leading to missing energy signatures. In section 4 we then analyze how the properties of KK particles can be determined, and point out methods to discriminate the 6DSM from 5DSM and supersymmetry. Section 5 is reserved for summary and discussion.

2. The six dimensional standard model

Universal extra dimensions (UED), in which all standard model fields propagate, have generated much interest due to opportunities for their discovery at collider and dark matter experiments. Precision electroweak constraints do not place very stringent constraints on the compactification scale of universal dimensions, allowing for new particles that are light enough to be accessible at the current generation of hadron colliders [1] (see [11] for review). Theories with universal extra dimensions have a Z_2 symmetry which is a remnant of the higher dimensional Lorentz symmetry. This Z_2 symmetry, called Kaluza-Klein parity, implies the lightest KK particle is stable and can be a good dark matter candidate.

6-dimensional UED models are particularly interesting since they provide elegant answers to various outstanding questions in the standard model. For instance anomaly cancellation in 6D can predict the existence of right-handed neutrinos and the correct number of fermion generations [13]. Proton stability can be attributed to what remains of the 6D Lorentz symmetry after compactification [14].

We consider two universal extra dimensions compactified on the chiral square, where two adjacent sides are identified [2, 3, 15]. KK particles are labeled by two positive inte-

JHEP02(2008)068

gers called 'level', (j,k), which represent quantization of momentum along the two extra dimensions. KK particles are odd under KK parity when $j+k$ is odd while they are even when $j+k$ is even, i.e. KK parity is defined as $(-1)^{j+k}$. Their tree-level masses are also determined by their level $M_{(j,k)} = \sqrt{j^2+k^2}/R$, where R is the radius of extra dimensions. This model gives rise to interesting collider phenomenology, due in part to the presence of new 'spinless adjoint' particles, the uneaten components of extra dimensional gauge fields. Furthermore not all KK masses are integer multiples of the compactification scale, level-2 KK particles ($(1,1)$ KK particles), for instance, have masses a factor $\sqrt{2}$ larger than the level-1 $(1,0)$ modes,[2] making the $(1,1)$ KK levels the most easily accessible new particles at the LHC [5].

The degeneracy of the modes of one level is lifted by one-loop mass corrections and by UV-generated boundary terms in a simple implementation of the 6-dimensional standard model on the chiral square, detailed in [2, 3, 15]. The 6DSM as an effective theory does not specify the coefficient of the boundary terms generated by the UV physics. However, since the one-loop mass terms from physics below the UV cutoff are enhanced by a logarithmic factor with respect to the UV boundary terms [4, 5], the latter are neglected throughout this work. Note that we choose a specific mass spectrum only for concreteness for our numerical analysis, but our main results do not depend very much on the precise values of the masses, as long as the hierarchy is not modified. The one-loop mass corrections result in the spinless adjoints becoming lighter than their corresponding gauge bosons [4] (different from 5DSM [16] due to existence of spinless adjoints). By forbidding decays to pure standard model final states, KK parity forces the (1,0) spinless adjoints to undergo 3-body decays via heavier $(1,0)$ fermions to pairs of standard model fermions and another $(1,0)$ mode. It also ensures the stability of the hypercharge spinless adjoint, the lightest KK-odd particle (LKP), making it a viable dark matter candidate [8] (see [17, 18] for comparison with 5-dimensional case). Level (1,0) modes pair produced at colliders therefore cascade decay via spinless adjoints to the LKP, resulting in events with large numbers of leptons and missing energy, a very distinctive signal at hadron colliders. Moreover a non-negligible fraction of multi-lepton events also contain photons from one-loop two-body decays of the level (1,0) hypercharge gauge boson [6]. The Feynman rules and mass spectrum are given in [3, 5, 6]. Following the notation in these references, we denote the spinless adjoints as $B_H^{(\mathbf{1})}$ for the U(1) hypercharge group and $Z_H^{(\mathbf{1})}$ and $W_H^{(\mathbf{1})\pm}$ for the $\mathrm{SU}(2)_W$ weak group, respectively.

The lowest level (1,0) of KK particles cannot decay into SM particles only, due to conservation of KK parity, so that they can only be produced in pairs. Higher level KK states with even KK parity, such as level (2,0) and (1,1) modes, on the other hand, can couple to SM particles. However, since this kind of coupling violates KK number, it is only mediated through loop-suppressed boundary terms (see for example [5]). As a result, level (2,0) or (1,1) states can be produced singly at colliders, but with relatively small cross sections.

The loop integrals for the mass terms and KK-number violating couplings are ultraviolet-divergent and need to be regularized by a cut-off. The cut-off scale Λ is estimated by naive dimensional analysis to be $\Lambda \sim 10 \times R^{-1}$ [5].

[2]We denote (1,0) state by (**1**) for brevity, especially when it appears as a particle index

JHEP02(2008)068

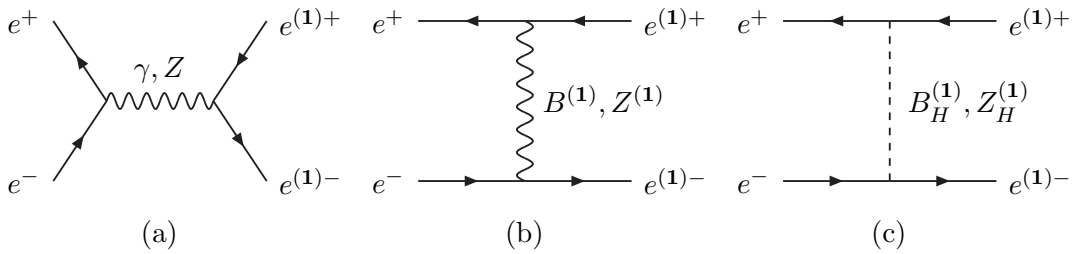

Figure 1: The tree-level Feynman diagrams for KK electron production, $e^+e^- \to e^{(1)+}e^{(1)-}$.

3. Production and decays of (1,0) particles at the ILC

In this section we will consider the production of (1,0) particles in the 6DSM at the ILC with $\sqrt{s} = 1\,\text{TeV}$ as well as their decays. Previously, detailed studies for level-1 KK-particles have been performed in the context of the 5DSM [19, 20]. One of the main differences between the 6DSM and the 5DSM are the presence of spinless adjoints. Nevertheless, some of our results are similar to the 5DSM case due to numerically negligible effects of spinless adjoints or their absence in certain processes. However, the one-loop corrected mass spectrum (see [16] and [4, 5] for comparison) is different, and production of spinless adjoints at the ILC is a new feature of the 6DSM beyond the 5DSM. Furthermore, previous studies of UED scenarios at linear colliders have focused on center-of-mass energies of several TeV. Therefore it is worth doing a complete analysis in the context of the 6DSM. For our study we have implemented the relevant interactions and 1-loop corrected masses of (1,0) particles in the 6DSM in `CalcHEP/CompHEP` [21 – 23] (see [24] for our model file). Since we want to compare the signatures with supersymmetry, we are also making use of the MSSM model file with a neutralino or gravitino as lightest supersymmetric particle (LSP) for `CalcHEP/CompHEP` [25].

Considering the bounds from searches at the Tevatron [6], which require $R^{-1} \gtrsim 300\,\text{GeV}$, it is very unlikely that a 500 GeV e^+e^- collider could observe any of the KK particles in this model. Therefore in this work we will focus on a 1 TeV version of the ILC. However, one should keep in mind that localized boundary terms from UV-completion physics, which are neglected here, could introduce additional mass splittings between the KK states. As a result, some KK particles can be lighter than 250 GeV, without violating the Tevatron limits. We will not explore this possibility further here.

3.1 KK fermions

We first turn to the discussion of (1,0) KK leptons. The (1,0) muons are produced via s-channel diagrams only (see figure 1a).[3] KK muons with $\mu^+\mu^- + \not{E}$ signature have been greatly studied in [19, 20] in the context of the 5DSM, exhibiting a clear difference in the

[3] In principle there are also s-channel diagrams with higher KK modes [19]. However their couplings to the standard model particles are 1-loop suppressed and their contributions are only important when the center-of-mass energy is close to the threshold. Higher KK bosons in the 6DSM turn out to be almost lepto-phobic [5].

JHEP02(2008)068

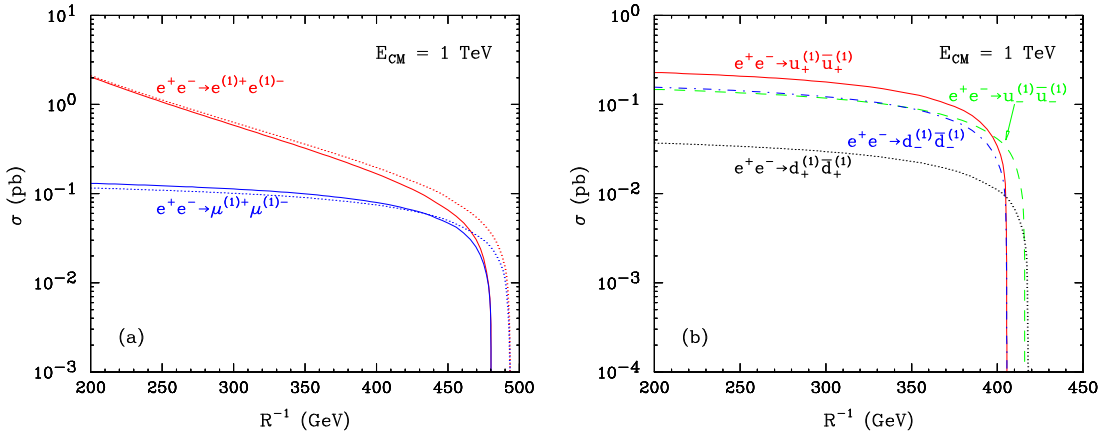

Figure 2: ISR-corrected production cross sections of (a) (1,0) KK leptons ($e^{(1)}$ in red $\mu^{(1)}$ in blue) and (b) (1,0) KK quarks, as a function of R^{-1}. Solid (dotted) lines correspond to $SU(2)_W$-doublets (singlets).

angular distributions of the final state muons in comparison with supersymmetry. KK tau-leptons are similar but can be observed in several modes depending on different τ decay channels. However, unlike the 5DSM where both $SU(2)_W$ singlet and doublet KK leptons always decay into a standard model lepton and the LKP B^1_μ, in the 6DSM a doublet (1,0) KK lepton can decay into one of several lighter (1,0) particles: 47% of the time for $W_H^{(1)\pm}$, 23.5% for $Z_H^{(1)}$ (which is equivalent to $W_H^{(1)3}$ due to the small Weinberg angle for KK states), 20% of the time for $B_H^{(1)}$, and only 9.3% for $B_\mu^{(1)}$ [6]. Using formulas for the decay withs of KK-leptons given in [6], we found that the singlet (1,0) lepton decays into $B_H^{(1)}$ 81% of the time and into $B_\mu^{(1)}$ with 19% branching fraction. The existence of spinless adjoints in this model greatly diversifies the decay modes of KK leptons, leading to richer phenomenology. For instance, a (1,0) KK-lepton can decay into $B_\mu^{(1)}$ plus a lepton, with the $B_\mu^{(1)}$ continuing to decay into $B_H^{(1)}$ emitting two leptons or a photon.

The case of (1,0) electrons is more interesting. Their production can also proceed through the t-channel diagrams as shown in figures 1b and 1c, leading to larger cross sections. The pair production cross section for (1,0) leptons are shown in figure 2. We found that diagrams with t-channel spinless adjoints contribute little to the total cross section. Angular distributions and spin correlations can provide important information about the spins of the particles in the t-channel and in the decays, and thus allow to discriminate this model from 5DSM or supersymmetry. However, due to the kinematics of the dominant t-channel exchange, the final state level-0 electron preferably goes in the forward direction, thus partially obscuring the spin correlation effects. On the other hand, utilizing polarized e^+ or e^- beams allows us to obtain additional information about the spin structure (see ref. [26] for a review on the role of polarized beams at ILC), as will be discussed in more detail in the next section.

KK quarks are produced in the same way as KK muons through photon and Z exchange in the s-channel. In the 5DSM, doublet and singlet KK quarks have different decay patterns: singlet KK quarks always decay into the B^1_μ LKP while the doublet KK quarks

JHEP02(2008)068

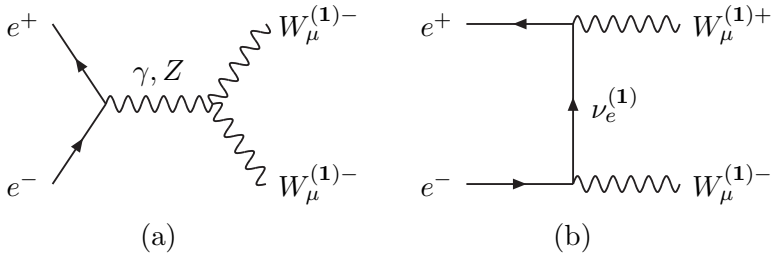

Figure 3: The tree-level Feynman diagrams for $W_\mu^{(1)-}W_\mu^{(1)+}$ production

decays into $W_\mu^{1\pm}$ or Z_μ^1. In the 6DSM, the dominant decay modes of both singlet and doublet KK quarks are into $G_H^{(1)}$ (see table 3 in [6] for branching fractions). The production cross sections of KK quarks plotted in figure 2b are of the same order as for KK-muons, but show a somewhat lower mass reach than for the case of KK leptons, since the KK-quarks receive large positive mass corrections. KK quark production is the only way to study the properties of the $G_H^{(1)}$ spin-0 color-octet at the ILC, since the decay of KK quarks is the only way to produce it at lepton colliders.

3.2 KK Bosons

The ISR-corrected production cross sections for (1,0) electroweak gauge bosons are shown in figure 4a. The production mechanism is identical to that in the standard model, replacing the standard model fermion with the corresponding KK mode, for example, as shown in figure 3 for $W_\mu^{(1)\pm}$ production (there are no s-channel diagrams for the production of neutral bosons). The branching fractions of the weak gauge bosons ($W_\mu^{(1)\pm}$ and $Z_\mu^{(1)}$ ($W_\mu^{(1)3}$)) are the same as those in the 5DSM (100% to $\mathrm{SU}(2)_W$ doublet leptons). However, while in the 5DSM the KK hypercharge gauge boson (B_μ^1) is stable, in the 6DSM the $B_\mu^{(1)}$ decays into the $B_H^{(1)}$ and SM particles. It decays into a photon plus $B_H^{(1)}$ 34% of the time, and into two leptons plus $B_H^{(1)}$ with 21.3% branching fraction per generation. This resembles the phenomenology of the lightest neutralino with a gravitino LSP. The pair production cross section for $B_\mu^{(1)}$ is relatively large, $\sim 100\,\mathrm{fb}$ for $R^{-1} \lesssim 500\,\mathrm{GeV}$. We will discuss the $2\gamma + \not{E}$ signature in the next section in detail.

Another important distinction is the production of spinless adjoints, for which we show our results in figure 4b. Production of $W_H^{(1)+}W_H^{(1)-}$ is mediated by photon and Z exchange in the s-channel and KK-neutrino exchange in the t-channel, as in the case of $W_\mu^{(1)+}W_\mu^{(1)-}$, while only t- or u-channel diagrams contribute for neutral bosons. The spinless adjoints have rather small cross sections except for charged pair production, due to the s-channel contribution. As a result of the approximate degeneracy in the mass spectrum, two-body decays are not allowed and the main decay mode of weak spinless adjoints is into lepton pairs plus $B_H^{(1)}$.

In figure 5 we summarize the decay patterns of (1,0) particles of the 6DSM in a pictorial way in comparison with the 5DSM [27]. There are two separate groups of particles: one (left in red) arising in both 5DSM and 6DSM, and the other (right in blue) that exists

JHEP02(2008)068

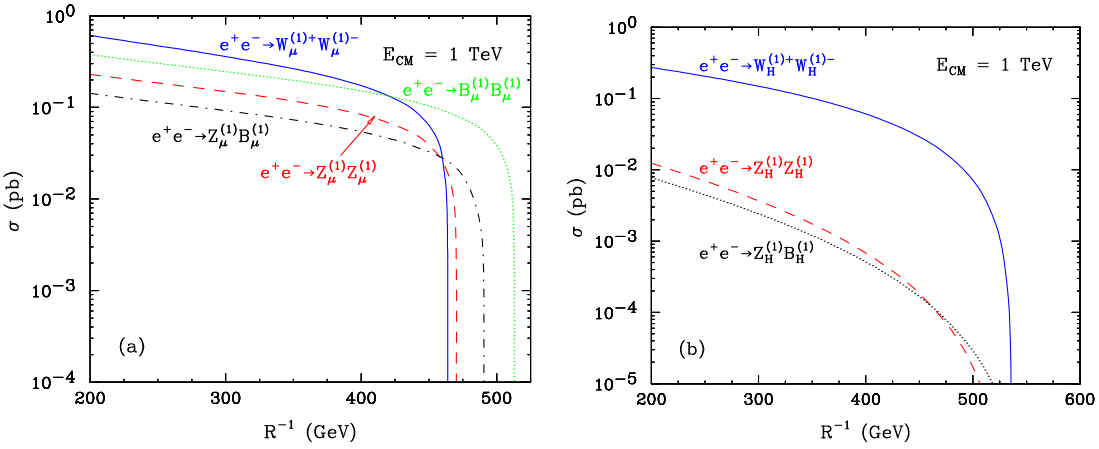

Figure 4: ISR-corrected production cross sections of (a) (1,0) KK vector bosons and (b) (1,0) spinless adjoints, as a function of R^{-1}.

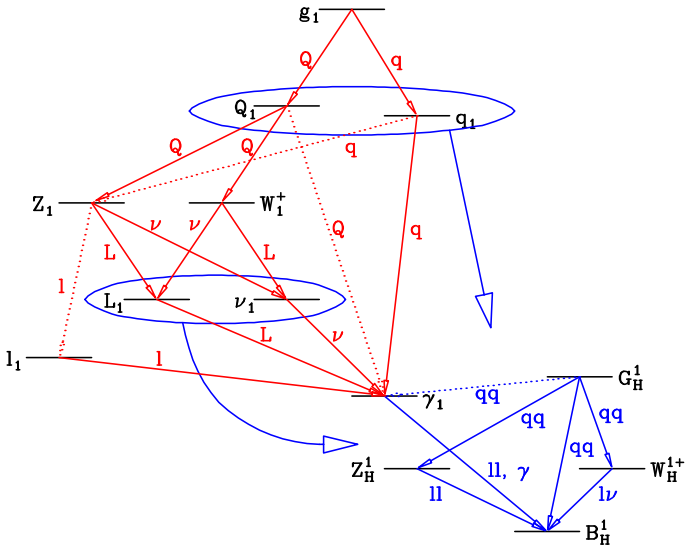

Figure 5: Schematic diagram for the decays of (1,0) KK particles. The typical particle spectrum and decay patterns of the 5DSM are shown in red, while the 6DSM encompasses the particles and decay modes depicted both in red and blue.

only in the 6DSM. These additional states are all spinless adjoints that are lighter than the $B_\mu^{(1)}$. One important consequence of this is that (1,0) fermions (circled) decay into these spinless adjoints with non-negligible branching fractions, thus completely changing the collider phenomenology.

4. Determination of particle properties and discrimination between 5DSM and 6DSM

In this section we consider specific signatures involving leptons and photons that are produced in the decay of electroweak (1,0) particles.

JHEP02(2008)068

4.1 Spin determination in KK-Lepton production and decays

In 5DSM, the lightest KK-odd particle (LKP) is typically a vector boson ($B_\mu^{(\mathbf{1})}$) while in 6DSM it is a scalar ($B_H^{(\mathbf{1})}$). For testing and discriminating these models it is therefore essential to determine the spin of the LKP.[4] This can be done by studying the decays of KK-electrons, as will be discussed in this section. The KK-excitations of right-handed electrons, $e_-^{(\mathbf{1})}$, decay directly into $B_\mu^{(\mathbf{1})}$ or $B_H^{(\mathbf{1})}$ and an electron. Therefore the pair production of $e_-^{(\mathbf{1})+}e_-^{(\mathbf{1})-}$ gives a very simple signature of e^+e^- and missing energy. By looking at the angular correlations of the final state e^+/e^-, one can learn something about the spin of the unreconstructed LKP. The use of polarized beams plays an important role here, as will be shown in the following.

For instance, one can study pair production of KK-electrons, $e_-^{(\mathbf{1})+}e_-^{(\mathbf{1})-}$, near their kinematical threshold. In this case, the KK-electrons are produced almost at rest. Owing to the t-channel diagrams for the pair production process, the production cross section is enhanced for a right-handed polarized electron beam, and a left-handed polarized positron beam. In this case, the initial e^+e^- state has a total spin of 1, so that the two produced KK-electrons need to have a combined total spin pointing in the same direction (the direction of the incoming e^-). Due to the helicity structure of the KK-electron couplings, the decay $e_-^{(\mathbf{1})\pm} \to e^\pm B_\mu^{(\mathbf{1})}$ produces left-handed electrons (right-handed positrons) for transverse polarization of the $B_\mu^{(\mathbf{1})}$, whereas $e_-^{(\mathbf{1})\pm} \to e^\pm B_H^{(\mathbf{1})}$ leads to right-handed electrons (left-handed positrons). As a consequence, angular momentum conservation mandates that for the decay into $B_\mu^{(\mathbf{1})}$, the outgoing e^- goes preferentially in the backward direction with respect to the incoming e^- beam, whereas for the decay into the scalar $B_H^{(\mathbf{1})}$, the e^- dominantly goes in the forward direction.

In the following, we will be studying three cases:

6DSM: a scenario of a model with two universal extra dimensions and $R^{-1} = 300\,\text{GeV}$. The masses and branching ratios of the KK-electrons and hypercharge bosons in this scenario are

$$
\begin{aligned}
M_{B_\mu^{(\mathbf{1})}} &= 292.0\ \text{GeV}, && \\
M_{B_H^{(\mathbf{1})}} &= 256.5\ \text{GeV}, && \\
M_{e_-^{(\mathbf{1})}} &= 304.5\ \text{GeV}, && \text{BR}[e_-^{(\mathbf{1})-} \to e^- B_\mu^{(\mathbf{1})}] = 19\%, \\
\Gamma_{e_-^{(\mathbf{1})}} &= 0.040\ \text{GeV}, && \text{BR}[e_-^{(\mathbf{1})-} \to e^- B_H^{(\mathbf{1})}] = 81\%, \\
M_{e_+^{(\mathbf{1})}} &= 312.0\ \text{GeV}, && \text{BR}[e_+^{(\mathbf{1})-} \to e^- B_\mu^{(\mathbf{1})}] = 12\%, \\
\Gamma_{e_+^{(\mathbf{1})}} &= 0.038\ \text{GeV}, && \text{BR}[e_+^{(\mathbf{1})-} \to e^- B_H^{(\mathbf{1})}] = 27\%, \\
& && \text{BR}[e_+^{(\mathbf{1})-} \to e^- W_H^{(\mathbf{1})0}, \nu_e W_H^{(\mathbf{1})-}] = 60\%.
\end{aligned}
\tag{4.1}
$$

[4] In general, the production cross sections are different between the models and may be used as a discriminator. However, the cross sections and branching fractions depend sensitively on the spectrum of the complete model. In this study we instead focus on spin determination from shape information of the final state distributions, which does not require reconstruction of the whole mass spectrum of the model.

JHEP02(2008)068

Since the $B_\mu^{(\mathbf{1})}$ is heavier than the $B_H^{(\mathbf{1})}$, it will decay into the latter plus a photon or a pair of leptons. By demanding a final state with a electron-positron pair and missing energy only, one can therefore select a sample of events which practically only contains direct decays to the LKP $B_H^{(\mathbf{1})}$.

5DSM: a scenario of a model with one universal extra dimensions with KK-electron and KK-B-boson masses chosen to match the kinematics of the 6DSM scenario:

$$\begin{aligned} M_{B_\mu^{(\mathbf{1})}} &= 256.5 \text{ GeV}, \\ M_{e_-^{(\mathbf{1})}} &= 304.5 \text{ GeV}, & \text{BR}[e_-^{(\mathbf{1})-} \to e^- B_\mu^{(\mathbf{1})}] &= 100\%, \\ \Gamma_{e_-^{(\mathbf{1})}} &= 0.11 \text{ GeV}, \\ M_{e_+^{(\mathbf{1})}} &= 312.0 \text{ GeV}, & \text{BR}[e_+^{(\mathbf{1})-} \to e^- B_\mu^{(\mathbf{1})}] &= 33\%, \\ \Gamma_{e_+^{(\mathbf{1})}} &= 0.11 \text{ GeV}, & \text{BR}[e_+^{(\mathbf{1})-} \to e^- W_\mu^{(\mathbf{1})0}, \nu_e W_\mu^{(\mathbf{1})-}] &= 67\%. \end{aligned} \tag{4.2}$$

SUSY: for completeness, we also consider a MSSM scenario, where the masses of the selectrons and neutralinos have been chosen to be equal to the masses of the KK-electrons and -bosons in the 6DSM scenario.

$$\begin{aligned} M_{\tilde{\chi}_2^0} &= 292.0 \text{ GeV}, \\ M_{\tilde{\chi}_1^0} &= 256.5 \text{ GeV}, \\ M_{\tilde{e}_R} &= 304.5 \text{ GeV}, & \text{BR}[\tilde{e}_R \to e^- \tilde{\chi}_1^0] &= 100\%, \\ \Gamma_{\tilde{e}_R} &= 0.13 \text{ GeV}. \end{aligned} \tag{4.3}$$

The contribution of the L-selectron has been disregarded in the SUSY scenario, since it can be significantly heavier than the R-selectron.

Idealized picture: no background, 100% polarization. We have generated signal cross sections and distributions for the three cases with `CompHEP 4.4` and `CalcHEP 2.5`. In a first step, only the signal process without backgrounds and with 100% polarization is considered.

As can be seen in figure 6a, near the production threshold of $2 \times 304.5\,\text{GeV} = 609\,\text{GeV}$, the 6DSM process with scalar adjoints in the final state is dominantly emitting the e^- in the forward direction, while the differential cross section vanishes in the backward direction.

On the other hand, in the 5DSM case where the LKP is a vector, the final state electron prefers to go in the backward direction. Due to the contribution of longitudinally polarized $B_\mu^{(\mathbf{1})}$ bosons, this is however a relatively small effect. Finally, for the case of supersymmetry (SUSY), the angular distribution is exactly flat owing to scalar nature of the selectrons, see figure 6a.

Since a future e^+e^- collider will spend most time running at specific design center-of-mass energies, it is interesting to see how much of these spin dependence effects survive at higher values of $\sqrt{s}$, i.e. not close to the threshold. This is shown in figure 6b. Due to the sizable boost of the heavy electron partners (KK-electrons or selectrons) the angular

JHEP02(2008)068

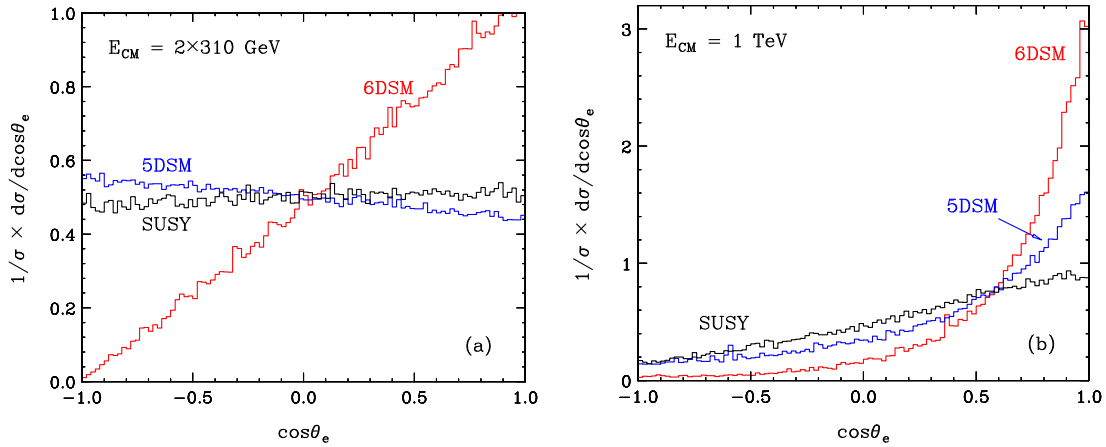

Figure 6: Angular dependence of the decay electron originating from pair production of heavy right-handed electron partners for 100% polarized $e^-_{\rm R}$ and $e^+_{\rm L}$ beams (a) near their production threshold and (b) at higher center-of-mass energy $\sqrt{s} = 1\,\text{TeV} \gg 2 \times m_{\text{epartner}}$. These plots compare three extensions of the standard model, where the heavy electron partners decays into an electron plus a stable weakly interacting particle. This stable particle can be a scalar (6DSM: $e^+e^- \to e^{(\mathbf{1})+}_+ e^{(\mathbf{1})-}_- \to e^+e^- B^{(\mathbf{1})}_H B^{(\mathbf{1})}_H$), vector (5DSM: $e^+e^- \to e^{1+}_+ e^{1-}_- \to e^+e^- B^1_\mu B^1_\mu$) or Majorana fermion (SUSY: $e^+e^- \to \tilde{e}_R \tilde{e}^*_R \to e^+e^- \tilde{\chi}^0_1 \tilde{\chi}^0_1$). The distributions are normalized to unity.

distributions for all models get deformed toward the forward region. Nevertheless, a sizable difference between the three cases remains. More information can be gained by also looking at the energy distribution of the final state e^+/e^-. Again as a result of the scalar nature of the selectron, the final state electron energy distribution in the SUSY case is perfectly flat, with a minimum and maximum given by the selectron and neutralino masses

$$E_{\text{min,max}} = \frac{\sqrt{s}}{4} \frac{m^2_{\tilde{e}} - m^2_{\tilde{\chi}^0_1}}{m^2_{\tilde{e}}} \left(1 \pm \sqrt{1 - \frac{4m^2_{\tilde{e}}}{s}}\right). \tag{4.4}$$

Since these lower and upper endpoints are defined solely through kinematics, they are identical for all three models (5DSM, 6DSM and SUSY), provided that the partners of the electrons and gauge bosons have the same masses in all models.

However, the forward peak due to angular correlations in the 6DSM model leads to a peak at the upper end of the electron energy distribution, see figure 7. The reason is that the forward direction of the electron corresponds to the upper end of its energy distribution, since in this kinematical configuration the boost of the KK-electron and the momentum of the electron are collinear. On the other hand, the electron energy distribution for the 5DSM model exhibits a slight slope toward the lower end.

Realistic picture: standard model backgrounds and realistic beam polarization. In the following, we assume 80% polarization of the elecron beam and 50% polarization of the positron beam. As pointed out above, right-handed e^- polarization and left-handed e^+ polarization enhance the signal of $e^{(\mathbf{1})+}_- e^{(\mathbf{1})-}_-$ production. In addition, this polarization combination also suppresses standard model background from W^+W^- production.

JHEP02(2008)068

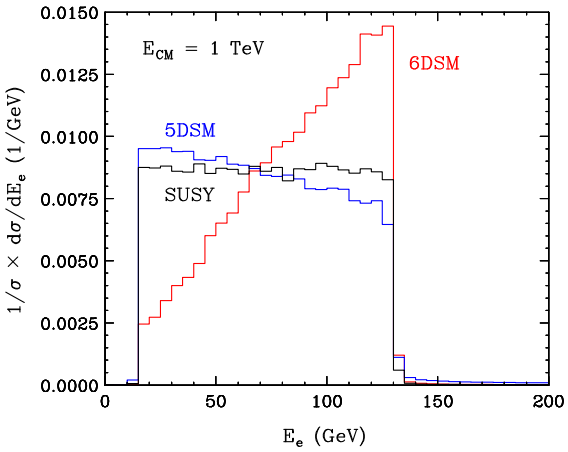

Figure 7: Energy dependence of the decay electron originating from pair production of heavy right-handed electron partners, for 100% polarized e^-_R and e^+_L beams. The notation is as in figure 6.

Without cuts, standard model backgrounds can be large and overwhelm the signal. The main standard model backgrounds for the signature of $e^+e^- + \not{E}$ (where $\not{E}$ stands for missing energy) come from the processes $e^+e^- \to e^+e^-\nu_e\nu_e$ (which includes W^+W^- and ZZ production) and $e^+e^- \to e^+e^-\gamma\gamma \to e^+e^-e^+e^-$. In the second process, the incoming e^+/e^- each radiate a near-collinear photon and proceed down the beam pipe. The two photons collide and generate an e^+e^- pair that is seen in the detector, while a missing energy signature is created by a small but non-negligible $p_\perp$ kick of the $e^\pm$ that are lost in the beam pipe.

In the following these standard model backgrounds are studied and it is shown how they can be reduced with simple selection cuts. To parametrize the detector acceptance, we demand the detected e^+ and e^- have a polar angle $\theta_{e^\pm}$ in the central detector region, $|\cos\theta_{e^\pm}| < 0.9$, a minimum energy $E_{e^\pm} > 5\,\text{GeV}$ and pair invariant mass $m_{ee} > 10\,\text{GeV}$. For the two-photon background we assume that the blind region around the beam pipe extends to 5° (87 mrad).

With this setup one finds the cross sections in the second line of table 1. Note that the standard model backgrounds are ill-defined without the minimal detector acceptance cuts, since they would diverge due to t-channel singularities.

Even without any selection cuts, the expected UED signal is already of the same order as the standard model backgrounds. In the SUSY case, however, the cross section is smaller, and thus we will apply additional cuts that are sufficient to ensure a clean SUSY signal.

Due to the heavy particles involved in the signal processes, they lead to larger values for the missing energy and the e^+e^- invariant mass than the standard model backgrounds. Therefore we apply the cuts $\not{E} > 0.7\sqrt{s}$ and $m_{ee} > 100\,\text{GeV}$. Furthermore, a lower limit on the total transverse momentum, $p_\perp > 10\,\text{GeV}$ (where the electron momenta have been summed vectorially), is effective against the two-photon background. After cuts one obtains the cross sections in the last line of the table 1.

The angular and energy distributions after cuts are shown in figure 8. The signal

JHEP02(2008)068

	Signal $e^+e^- B_H^{(1)} B_H^{(1)}$	$e^+e^- B_\mu^{(1)} B_\nu^{(1)}$	$e^+e^- \tilde{\chi}_1^0 \tilde{\chi}_1^0$
No cuts	1.18(3) pb	2.42(2) pb	116(2) fb
Acceptance cuts	0.646(15) pb (55%)	1.61(2) pb (66%)	98(2) fb (85%)
Selection cuts	0.518(2) pb (44%)	0.703(3) pb (29%)	53.9(4) fb (46%)

	Background $e^+e^-\nu_e\nu_e$	$\gamma\gamma \to e^+e^-$
Acceptance cuts	9.07(8) fb	1.5(2) pb
Selection cuts	0.263(2) fb	3.9(2) fb

Table 1: Top: cross sections for 6DSM, 5DSM and SUSY signals stemming from KK-electron/selectron production. Bottom: relevant standard model backgrounds.

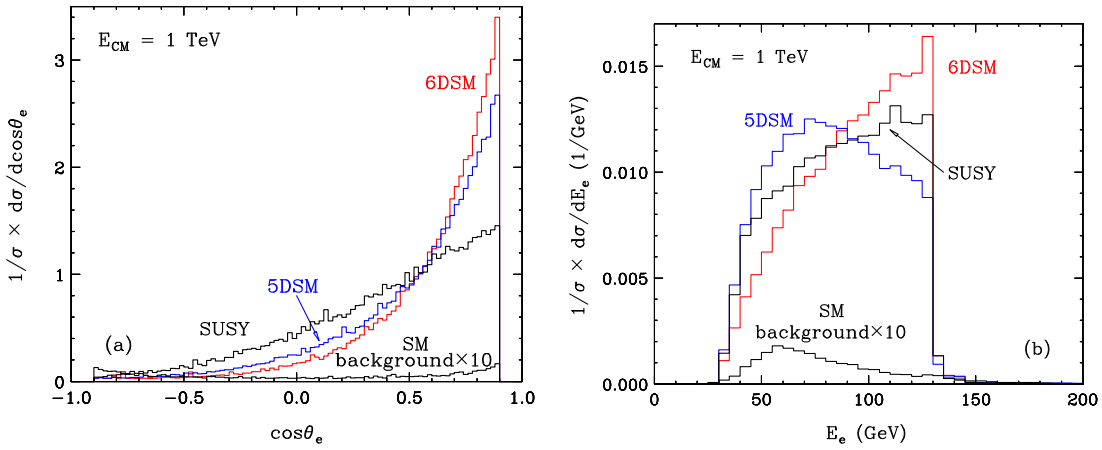

Figure 8: (a) Angular distribution and (b) energy distribution of the decay electron originating from pair production of heavy right-handed electron partners at $\sqrt{s} = 1\,\text{TeV}$, after application of cuts to reduce standard model background. The distributions have been normalized to unity for the three new physics models. Also shown is the standard model background for the 6DSM case, scaled by a factor 10 to make it visible.

cross sections have been normalized to unity, while the standard model background has been scaled in the same way as the 6DSM signal cross section, i.e. the figure reflects the signal-to-background ratio that is expected for the 6DSM. It can be seen that for the large expected signal cross sections in the UED scenarios the standard model background is totally negligible. While the shape of the angular distribution is not affected by the selection cuts, the energy distribution is distorted near its lower end. Nevertheless, a clear distinction between the three models is possible from the upper end of the energy distribution.

Assuming $500\,\text{fb}^{-1}$ luminosity at $\sqrt{s} = 1\,\text{TeV}$, and a signal cross section of 518 fb (which corresponds to the 6DSM case) for all three models (6DSM, 5DSM and SUSY), the 5DSM and 6DSM spin structure can be distinguished by about 12 standard deviations from the angular distribution shape. Here only statistical errors have been taken into account, using a binned χ^2 test. The SUSY spin assignments can be discriminated from the 6DSM

JHEP02(2008)068

case by about 37 standard deviations. When instead considering the energy distributions, 5DSM and 6DSM can be separated by about 32 standard deviations, while SUSY and 6DSM can be distinguished by 18 standard deviations.

In other words, for a separation of the three scenarios at 95% confidence level, $2\,\text{fb}^{-1}$ luminosity at $\sqrt{s} = 1\,\text{TeV}$ is sufficient. Even if the cross section after cuts is only 54 fb, as in the SUSY case, $19\,\text{fb}^{-1}$ luminosity suffices for the discrimination.

4.2 Photonic decays of hypercharge bosons

As discussed in section 3.2, $B_\mu^{(\mathbf{1})}$ pairs are produced through $e_+^{(\mathbf{1})}$ and $e_-^{(\mathbf{1})}$ exchange in the t-channel while $\tilde{\chi}_0^1$ pair production is mediated by s-channel Z boson as well. In the 6DSM, they can decay into a photon plus the invisible LKP, $B_H^{(\mathbf{1})}$, with a sizable branching fraction of 34% [6]. Thus they lead to the characteristic final state signature of two photons plus missing energy, $2\gamma + \not{E}$. A very similar signal can originate from supersymmetry with a light gravitino $\tilde{G}$, which is common for example in gauge mediated supersymmetry breaking (GMSB). In this case, the lightest neutralino $\tilde{\chi}_0^1$, if it is the NLSP, always decays to $\tilde{G}$ and a photon. Assuming ignorance about the mass spectrum of the two models, 6DSM and GMSB, the only difference are the spins of the particles involved.

In the following we study how GMSB and 6DSM can be distinguished in the $2\gamma + \not{E}$ signal by analyzing the decay distributions of the photons. In figure 9, we show the energy and angular distribution of the photons, after applying suitable cuts ($E_\gamma > 5\,\text{GeV}$ and $|\cos\theta_\gamma| < 0.9$) to ensure that the photons are visible in the detector. As shown in figure 4, the signal cross section for $B^{(\mathbf{1})}$-pair production is of the order of ∼100 pb up to $R^{-1} \lesssim 500\,\text{GeV}$, which is about 5 times larger than the $\tilde{\chi}_0^1\tilde{\chi}_0^1$ production cross section for equal masses. The efficiency due to the two cuts above is high (about 78% for $R^{-1} = 300\,\text{GeV}$). The main SM background to $2\gamma + \not{E}$ comes from $\gamma\gamma Z$ with invisible Z decay, whose cross section is about $16\,\text{fb} \times 0.2 = 3.2\,\text{fb}$ after cuts, and thus already much smaller than the expected signal. Furthermore, the photon energy distribution in 6DSM and GMSB has distinct kinematic endpoints, which are given by a formula analogous to eq. (4.4). Unlike this, the energy spectrum of the photon in the SM background is continuous and peaks at $E_\gamma \sim 0\,\text{GeV}$ or $E_\gamma \sim 500\,\text{GeV}$. Using this fact together with a proper cut on the invariant mass of the two photons, this background becomes completely negligible (smaller by more than 6 orders of magnitude).

From the right frame of figure 9 we conclude that the photons in GMSB tend to be more central while in 6DSM they preferably go in the forward or backward direction. This is due to the behavior of the mother particles when they are produced from e^+e^- collision, i.e. vector bosons ($B_\mu^{(\mathbf{1})}$) prefer the forward or backward direction and neutralinos ($\tilde{\chi}_0^1$) are produced more in the central region. This would allow for a clear discrimination of the two models based on the spins of the next-to-lightest new particles.

Note that the decay $B_\mu^{(\mathbf{1})} \to B_H^{(\mathbf{1})} + \gamma$ is mediated by loop diagrams, leading to the effective coupling [6]

$$-\frac{R}{4}\,\mathcal{C}_\text{B}\,\epsilon^{\mu\nu\rho\sigma} F_{\mu\nu} B_{\rho\sigma}^{(\mathbf{1})} B_H^{(\mathbf{1})}, \tag{4.5}$$

JHEP02(2008)068

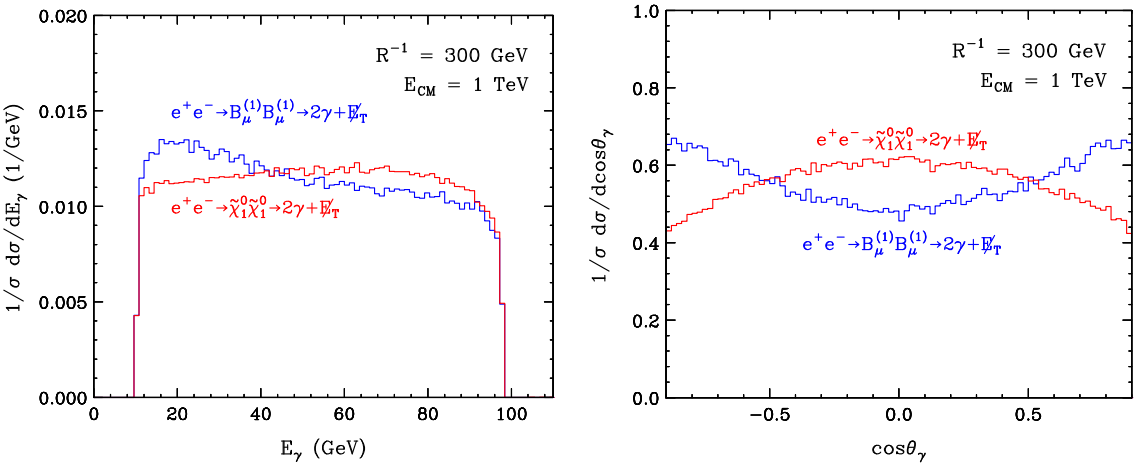

Figure 9: (a) Energy and (b) angular distributions of photon in $2\gamma + \not{E}$ for 6DSM and supersymmetry with gravitino dark matter

where $F_{\mu\nu}$ and $B^{(1)}_{\rho\sigma}$ are the field strengths of the photon and the KK hypercharge boson $B^{(1)}_\mu$, respectively. This interaction reflects the fact that the adjoint scalar $B^{(1)}_H$ is a pseudo-scalar, with $CP = -1$ quantum numbers. In contrast, CP-even scalars would couple to gauge bosons via

$$-\frac{R}{4}\,\mathcal{C}'_{\rm B}\,F^{\mu\nu}\,B^{(1)}_{\mu\nu}\,B^{(1)}_H. \tag{4.6}$$

This interaction does not exist in the 6DSM. It would be interesting to explore if these two cases can be distinguished experimentally by studying the process $e^+e^- \to B^{(1)}_\mu B^{(1)}_\mu \to \gamma\gamma\, B^{(1)}_H B^{(1)}_H$. However, an explicit calculation shows that both coupling types lead to the same squared matrix element, so that a discrimination is not possible.

This is quite unlike Higgs-strahlung, $e^+e^- \to Z\phi$, where a scalar or pseudo-scalar Higgs ϕ lead to very different angular distributions [28]. The crucial discriminative power here comes from the fact that for the scalar coupling, the longitudinal degree of freedom of the Z boson contributes, while for the pseudo-scalar coupling is does not. In the decay $B^{(1)}_\mu \to B^{(1)}_H + \gamma$, however, the photon has only transverse polarization states, so that the distinction between scalar and pseudo-scalar couplings disappears.

4.3 Discovery potential for (1,1) KK states

Beyond the lowest (1,0) or, equivalently, (0,1) KK excitations, the 6DSM also contains many particles with higher KK numbers. Of special interest are states which have non-zero KK number for each of the two extra dimensions. The lightest of these are the (1,1) excitations. Since boundary terms break KK number, and only KK parity is preserved exactly, the (1,1) states can be produced singly through the interaction of two standard model particles. The tree-level mass of the (1,1) particles is $m_{(1,1),\rm tree} = \sqrt{2}/R$, so that they are the lightest states that can be singly produced. In contrast, the (2,0) excitation have a mass of $m_{(2,0),\rm tree} = 2/R$, which is very similar to the level-2 states in the 5DSM. Therefore the existence of particles with even KK parity, but with a mass which is significantly smaller than $2/R$, is a unique feature of models with more than one universal extra dimension.

JHEP02(2008)068

This property can be used to distinguish 6DSM and 5DSM, in addition to the appearance of scalar adjoints.

In e^+e^- collisions, the (1,1) excitations of the neutral gauge bosons can be produced in the s-channel. In total, there are four (1,1) partners of the neutral vector bosons: the vector modes $B_\mu^{(1,1)}$ and $W_\mu^{(1,1)3}$, as well as the scalar adjoints $B_H^{(1,1)}$ and $W_H^{(1,1)3}$. The vectors couple to standard model fermions through the interactions [5]

$$\frac{g\xi_f^W}{16\pi^2}\log\frac{\Lambda^2R^2}{2}\;\bar{f}_{\rm L}\gamma^\mu I^3 f_{\rm L}\,W_\mu^{(1,1)3}, \qquad \frac{g'\xi_f^B}{16\pi^2}\log\frac{\Lambda^2R^2}{2}\;\bar{f}\gamma^\mu\frac{Y_f}{2}f\,B_\mu^{(1,1)}, \tag{4.7}$$

where I^3 and Y_f are the generators of the third component of weak $\mathrm{SU}(2)_W$ isospin and of hypercharge, respectively, and g and g' are the couplings of corresponding gauge groups. The ξ's are defined as

$$\xi_q^W = -4g_{\rm s}^2 - \frac{1}{2}(\lambda_u^2+\lambda_d^2) + \frac{11}{12}g^2 - \frac{1}{12}g'^2, \tag{4.8}$$

$$\xi_l^W = -\frac{1}{2}\lambda_l^2 + \frac{11}{12}g^2 - \frac{3}{4}g'^2, \tag{4.9}$$

$$\xi_{q_{\rm L}}^B = -4g_{\rm s}^2 - \frac{1}{2}(\lambda_u^2+\lambda_d^2) - \frac{9}{4}g^2 - \frac{83}{12}g'^2, \tag{4.10}$$

$$\xi_{q_{\rm R}}^B = -4g_{\rm s}^2 - \lambda_q^2 - \frac{43}{6}g'^2, \tag{4.11}$$

$$\xi_{l_{\rm L}}^B = -\frac{1}{2}\lambda_l^2 - \frac{9}{4}g^2 - \frac{91}{12}g'^2, \tag{4.12}$$

$$\xi_{l_{\rm R}}^B = -\lambda_l^2 - \frac{59}{6}g'^2. \tag{4.13}$$

Here $\lambda_u, \lambda_d, \lambda_l$ are the (generation-dependent) Yukawa couplings of the up-type quarks, down-type quarks and leptons, respectively, which except for λ_t can be neglected with good approximation.

The scalars couple to standard model fermions only through higher-dimensional terms [5]:

$$\frac{g\zeta_f^W}{16\pi^2(\sqrt{2}R^{-1})}\log\frac{\Lambda^2R^2}{2}\;\bar{f}_{\rm L}\gamma^\mu I^3 f_{\rm L}\,D_\mu W_H^{(1,1)3}, \qquad \text{etc.}, \tag{4.14}$$

with $\zeta_f^W \sim \mathcal{O}(g_{\rm s}^2, g^2)$. By using equations of motion, it can be seen that couplings of type eq. (4.14) are suppressed by the mass of the fermion f. Consequently, $B_H^{(1,1)}$ and $W_H^{(1,1)3}$ cannot be produced singly in significant rates at an e^+e^- collider.

In the following we concentrate on the production of (1,1) vector bosons. Since the interaction terms eq. (4.7) are suppressed by a loop factor, the widths of the (1,1) vectors in quite small. For example, for $R^{-1} = 300\,\mathrm{GeV}$ one obtains at one-loop level:

$$M_{B_\mu^{(1,1)}} = 415\ \mathrm{GeV}, \qquad \Gamma_{B_\mu^{(1,1)}} = 0.088\ \mathrm{GeV} \approx 2.1\times10^{-4} M_{B_\mu^{(1,1)}}, \tag{4.15}$$

$$M_{W_\mu^{(1,1)3}} = 465\ \mathrm{GeV}, \qquad \Gamma_{W_\mu^{(1,1)3}} = 0.20\ \mathrm{GeV} \approx 4.4\times10^{-4} M_{W_\mu^{(1,1)3}}. \tag{4.16}$$

Such narrow resonances in the s-channel are difficult to observe in e^+e^- collisions, unless by coincidence the center-of-mass energy is close to the mass of the resonances, $\sqrt{s} \approx$

JHEP02(2008)068

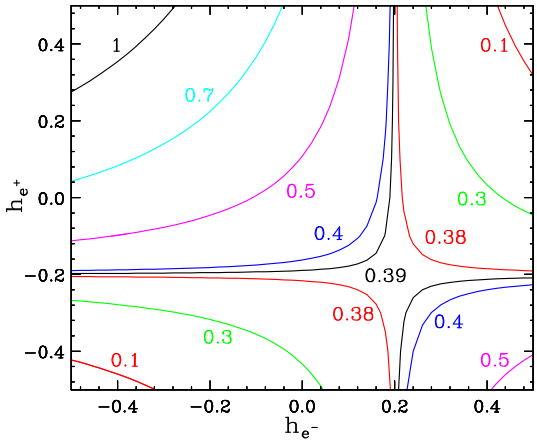

Figure 10: Cross section for $e^+e^- \to \gamma B_\mu^{(1,1)}$ in helicity basis with $E_\gamma > 5\,\text{GeV}$ and $|\cos\theta_\gamma| < 0.9$.

$M_{B_\mu^{(1,1)}}, M_{W_\mu^{(1,1)3}}$. If $M_{B_\mu^{(1,1)}}, M_{W_\mu^{(1,1)3}} < \sqrt{s}$, however, these particles can be produced via radiation of an additional photon,

$$e^+e^- \to V_\mu^{(1,1)} + \gamma, \tag{4.17}$$

where $V = B, W^3$. Figure 10 shows the cross section (in fb) for $e^+e^- \to B_\mu^{(1,1)} + \gamma$ in the helicity bases of the e^+e^- beams. Since initial-state radiation is dominated by collinear emission, the photon will be mostly lost unobserved in the beam pipe. Therefore one has to focus on the final state decay products of the $V_\mu^{(1,1)}$ in order to discriminate it from the standard model background. Both $B_\mu^{(1,1)}$ and $W_\mu^{(1,1)3}$ have very small couplings to standard model leptons, leading to suppressed branching fractions $\text{BR}[B_\mu^{(1,1)} \to e^+e^-] \approx 1\%$ and $\text{BR}[W_\mu^{(1,1)3} \to e^+e^-] \approx 0.015\%$. Thus a discovery in the leptonic final state channels does not appear promising. On the other hand, there are large branching fractions into jets (including all quark flavors except the top quark): $\text{BR}[B_\mu^{(1,1)} \to jj] \approx 70\%$ and $\text{BR}[W_\mu^{(1,1)3} \to jj] \approx 70\%$. Therefore, in spite of the limited precision for jet energy measurements, the di-jet final state is the most promising channel for discovering the (1,1) vector bosons.

The capability for finding a narrow vector resonance through the radiative return process eq. (4.17) has been analyzed in detail in ref. [29], including standard model backgrounds and detector resolution effects. Several run scenarios for an e^+e^- linear collider have been considered: *(1)* a scan at the WW pair production threshold $\sqrt{s} \approx 170\,\text{GeV}$ with $50\,\text{fb}^{-1}$ integrated luminosity, *(2)* a scan at the tt pair production threshold $\sqrt{s} \approx 350\,\text{GeV}$ with $100\ \text{fb}^{-1}$, *(3)* a first-stage high-energy run at $\sqrt{s} \approx 500\,\text{GeV}$ with $500\,\text{fb}^{-1}$, *(4)* and a second-stage run at $\sqrt{s} \approx 1000\,\text{GeV}$ with $1000\,\text{fb}^{-1}$. The estimated reach versus the predicted cross section is shown in figure 11. The figure has been normalized to the case of a vector boson with the same couplings as the standard model Z boson, however this normalization does not affect the conclusions.

As evident from the figure, a 1 TeV e^+e^- collider can discover the $B_\mu^{(1,1)}$ boson for any mass $M_{B_\mu^{(1,1)}} < 1\,\text{TeV}$. In addition, a measurement of the di-jet invariant mass will provide

JHEP02(2008)068

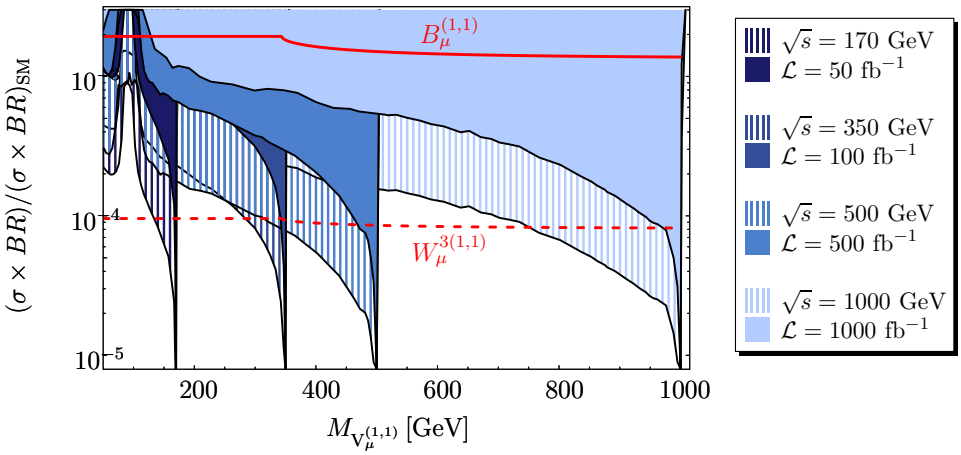

Figure 11: Projected sensitivity of ILC of $B_\mu^{(1,1)}$ and $W_\mu^{(1,1)3}$ for different run scenarios, as function of the (1,1) vector boson mass. The hatched regions correspond to the 95% confidence level exclusion reach, while the solid regions indicate the 5σ discovery reach.

a (moderately precise) determination of the $B_\mu^{(1,1)}$ boson mass. On the other hand, the $W_\mu^{(1,1)3}$ has a much smaller cross section owing to its smaller coupling to e^+e^-, so that a direct discovery of this particle would only be possible if the center-of-mass energy is close to its mass.

However, once a signal for the $B_\mu^{(1,1)}$ is detected, one could obtain more information by tuning the collider energy to its mass. Moreover, one could look for the $W_\mu^{(1,1)3}$ by setting the center-of-mass energy closely above $\sqrt{s} \approx 1.1 \times M_{B_\mu^{(1,1)}}$, where the $W_\mu^{(1,1)3}$ resonance is expected in the minimal 6DSM model.

By tuning the center-of-mass energy on the s-channel resonances of $B_\mu^{(1,1)}$ and $W_\mu^{(1,1)3}$, the masses, branching fractions and couplings ratios of these particles can be determined to the per-cent level with only a few fb^{-1} luminosity [29]. However, it will be very difficult to resolve the non-zero widths of these resonances, since they are comparable to the expected intrinsic beam energy spread of order $\mathcal{O}(10^{-4})$, and are further washed out by beam- and bremsstrahlung. A measurement of the total width of the (1,1) vector bosons would be very interesting, because it would allow to determine the absolute coupling strength and thus obtain an estimate of the scale Λ of the UV completion.[5] In principle, a determination of the absolute coupling strength of (1,1) vector bosons is feasible by measuring the invisible decay modes $B_\mu^{(1,1)}, W_\mu^{(1,1)3} \to \nu\bar{\nu}$ with the help of an initial-state photon for tagging [29]. However, the photon-tagging requirement strongly reduces the statistics for this kind of measurement, so that it would only be possible to establish an upper bound on the branching fractions of $B_\mu^{(1,1)}$ and $W_\mu^{(1,1)3}$ into neutrinos. Nevertheless, this would already allow a rough determination of the absolute coupling strength to the level of about 6% for the $B_\mu^{(1,1)}$ (This estimate was derived from the analysis in ref. [29]).

While, as pointed out above, the single production of the (1,1) spinless adjoints in e^+e^- collisons is highly suppressed, pair production of of these particles is not suppressed

[5] Admittedly, such an estimate of Λ would be highly model-dependent since non-perturbative boundary terms could modify eq. (4.7)

JHEP02(2008)068

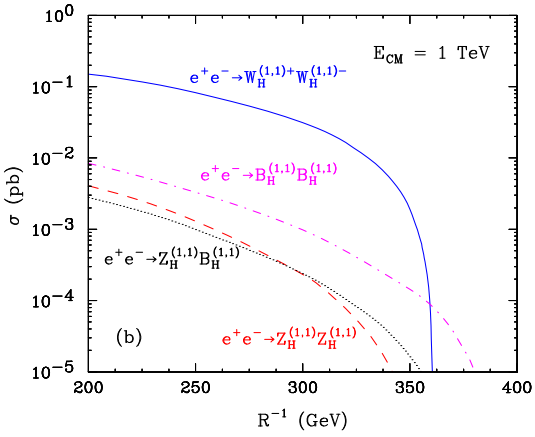

Figure 12: Pair production cross section for spinless adjoints of KK-level (1,1).

by the KK-number violating interaction. Their production mechanisms are exactly the same as for (1,0) pair production, as discussed in section 3.2, and the cross sections are large for low R^{-1}, as shown in figure 12. Once these two spinless adjoints are produced, they decay into the heaviest standard model fermion pair, if kinematically allowed. For instance, $Z_H^{(1,1)}$ and $B_H^{(1,1)}$ decay into $t\bar{t}$, and $W_H^{(1,1)+}$ decays into $t\bar{b}$.

For pair production of $Z_H^{(1,1)}$ or $B_H^{(1,1)}$ (or mixed $Z_H^{(1,1)} B_H^{(1,1)}$ pairs), $t\bar{t}t\bar{t} \to b\bar{b}b\bar{b}W^+W^-W^+W^-$ is expected in the final state. Up to $R^{-1} \sim 300\,\mathrm{GeV}$, from figure 12, at least a few tens of such events can be observed with a luminosity of $500\,\mathrm{fb}^{-1}$, which already can be sufficient for a discovery since the standard model background is extremely small. An interesting signature might be $\ell^\pm\ell^\pm + N$ jets $+ \not{E} + X$ with $N \geq 4$ and ℓ being e or μ. In order to reconstruct the mass of the $Z_H^{(1,1)}$ or $B_H^{(1,1)}$ from the decay products, the fully hadronic decay of two W's needs to be considered. The separate mass reconstruction of $Z_H^{(1,1)}$ and $B_H^{(1,1)}$, however, will be difficult due to combinatorial background from many jets and the fact that these two spinless adjoints are close in mass. Nevertheless a rough estimate of the overall mass scale can be made. This estimate could then be made more precise by tuning the center-of-mass energy near the threshold, allowing a separation of the two mass states. From a measurement of the β^3 behavior ($\beta = \sqrt{1 - 4m_{(1,1)}^2/s}$) of the cross section near threshold it could be confirmed that the produced particles are scalar.

For $W_H^{(1,1)+}W_H^{(1,1)-}$ production the signature is $t\bar{t}b\bar{b} \to b\bar{b}b\bar{b}W^+W^-$, with the dominant background being $t\bar{t}$ with two jets from final state radiation, which is expected to be small. Furthermore, the cross section for $W_H^{(1,1)+}W_H^{(1,1)-}$ is approximately one order of magnitude larger than the production cross section of the neutral scalars due to γ and Z exchange in the s-channel. An accurate mass measurement of $W_H^{(1,1)^\pm}$ could provide evidence that $W_H^{(1,1)^\pm}$ and $Z_H^{(1,1)}$ form an $\mathrm{SU}(2)_W$ triplet.

Unfortunately the reach of a 1 TeV ILC for the electroweak spinless adjoints is limited to $R^{-1} \lesssim 350\,\mathrm{GeV}$ due to the heaviness of the (1,1) states. Note that the final state signature for the electroweak spinless adjoints is quite similar to the (1,1) spinless adjoint of the gluon, which could be observable at hadron colliders [7].

JHEP02(2008)068

5. Conclusions

Universal extra dimensions are an attractive candidate for new physics, which would explain the naturalness of the electroweak scale. In contrast to the extension of the standard model by one extra dimension (5DSM), the standard model with two extra dimensions (6DSM) has elementary gauge bosons with six components, one of which becomes an independent scalar particle degree of freedom. These kind of particles are usually referred to as scalar adjoints. The first Kaluza-Klein excitation of the scalar adjoint of the hypercharge gauge group is expected to be the lightest Kaluza-Klein particles and thus would constitute a good dark matter candidate. Therefore, the 6DSM has a rich phenomenology at future colliders, with multi-lepton final states, since the KK-gauge bosons can decay into the corresponding scalar adjoints. Moreover, the scalar dark matter particle is different from supersymmetry and the 5DSM, where the new stable particle typically would be a fermion or vector boson, respectively. Other characteristic features of the 6DSM is the decay of the KK-level-1 hypercharge vector boson into the hypercharge scalar adjoint (which is the lightest KK particle, LKP) and a photon through a loop mediated interaction, and the presence of higher KK-states which have non-zero KK numbers for both extra dimensions. The lowest of the these states are the level (1,1) KK excitation, with a mass that is only larger by factor a $\sqrt{2}$ compared to the (1,0) states.

In this work, we have analyzed how these properties could be studied experimentally at a future e^+e^- collider such as ILC. We have computed the cross sections for the production of various KK particles at ILC with $\sqrt{s} = 1\,\text{TeV}$ as a function of the size R of the extra dimensions and discussed the decay pattern of each particle. The rates for many of the new particles are large enough to be observable at the ILC if they are within kinematical reach. We found that a clean determination of the LKP spin is possible in the production of KK-electrons, which decay into standard model electrons and the LKP.

In order to study the 1-loop decay of the KK hypercharge gauge boson into a photon, we implemented this interaction into `CalcHEP/CompHEP`, which will be useful for further studies. We were able to show that the signal for this decay is very clean at the ILC, and using the angular distribution, can be distinguished from the decay of neutralinos into gravitinos in gauge-mediated supersymmetry breaking. We further tried to find a method for determining the CP properties of the LKP, but found that the process does not have any sensitivity to the CP quantum numbers.

Finally, we have studied the production of (1,1) vector bosons and spinless adjoints. The vector bosons can be produced singly in e^+e^- collisions, but with rather small cross sections. Nevertheless, a discovery of the (1,1) hypercharge gauge boson is possible at the ILC, if its mass is smaller than the maximum center-of-mass energy of the collider. For the (1,1) spinless adjoints, the single-production cross sections are too small for an observation, but if light enough, they could be pair-produced in sizable rates.

In summary, if TeV-scale universal extra dimensions exist, the predicted KK excitations could be discovered at future colliders, leading to a rich and exciting phenomenology. At a high-energy e^+e^- collider, the spectrum, quantum numbers and decay patterns of the KK particles can be determined precisely, thus allowing a window into the underlying structure

JHEP02(2008)068

of the compactification.

Acknowledgments

We would like to thank B. Dobrescu and R. Mahbubani for useful discussions and helpful comments on the manuscript. ANL is supported by the U.S. Department of Energy, Division of High Energy Physics, under Contract DE-AC02-06CH11357. Fermilab is operated by Fermi Research Alliance, LLC under Contract No. DE-AC02-07CH11359 with the U.S. Department of Energy. During the early stages of the project, AF was supported by the Swiss Nationalfonds, and is grateful to the University of Zurich for the pleasant working environment during that time.

References

[1] T. Appelquist, H.-C. Cheng and B.A. Dobrescu, *Bounds on universal extra dimensions*, *Phys. Rev.* **D 64** (2001) 035002 [hep-ph/0012100].

[2] B.A. Dobrescu and E. Ponton, *Chiral compactification on a square*, *JHEP* **03** (2004) 071 [hep-th/0401032].

[3] G. Burdman, B.A. Dobrescu and E. Ponton, *Six-dimensional gauge theory on the chiral square*, *JHEP* **02** (2006) 033 [hep-ph/0506334].

[4] E. Ponton and L. Wang, *Radiative effects on the chiral square*, *JHEP* **11** (2006) 018 [hep-ph/0512304].

[5] G. Burdman, B.A. Dobrescu and E. Ponton, *Resonances from two universal extra dimensions*, *Phys. Rev.* **D 74** (2006) 075008 [hep-ph/0601186].

[6] B.A. Dobrescu, K. Kong and R. Mahbubani, *Leptons and photons at the LHC: cascades through spinless adjoints*, *JHEP* **07** (2007) 006 [hep-ph/0703231].

[7] B.A. Dobrescu, K. Kong and R. Mahbubani, *Massive color-octet bosons and pairs of resonances at hadron colliders*, arXiv:0709.2378.

[8] B.A. Dobrescu, D. Hooper, K. Kong and R. Mahbubani, *Spinless photon dark matter from two universal extra dimensions*, *JCAP* **10** (2007) 012 [arXiv:0706.3409].

[9] K. Hsieh, R.N. Mohapatra and S. Nasri, *Dark matter in universal extra dimension models: Kaluza-Klein photon and right-handed neutrino admixture*, *Phys. Rev.* **D 74** (2006) 066004 [hep-ph/0604154].

[10] K. Hsieh, R.N. Mohapatra and S. Nasri, *Mixed dark matter in universal extra dimension models with TeV scale $W(R)$ and Z'*, *JHEP* **12** (2006) 067 [hep-ph/0610155].

[11] D. Hooper and S. Profumo, *Dark matter and collider phenomenology of universal extra dimensions*, *Phys. Rept.* **453** (2007) 29 [hep-ph/0701197].

[12] I. Yavin, *A review of spin determination at the LHC*, *Mod. Phys. Lett.* **A 22** (2007) 2315.

[13] B.A. Dobrescu and E. Poppitz, *Number of fermion generations derived from anomaly cancellation*, *Phys. Rev. Lett.* **87** (2001) 031801 [hep-ph/0102010].

[14] T. Appelquist, B.A. Dobrescu, E. Ponton and H.-U. Yee, *Proton stability in six dimensions*, *Phys. Rev. Lett.* **87** (2001) 181802 [hep-ph/0107056].

JHEP02(2008)068

[15] M. Hashimoto and D.K. Hong, *Topcolor breaking through boundary conditions*, *Phys. Rev.* **D 71** (2005) 056004 [hep-ph/0409223].

[16] H.-C. Cheng, K.T. Matchev and M. Schmaltz, *Radiative corrections to Kaluza-Klein masses*, *Phys. Rev.* **D 66** (2002) 036005 [hep-ph/0204342].

[17] G. Servant and T.M.P. Tait, *Is the lightest Kaluza-Klein particle a viable dark matter candidate?*, *Nucl. Phys.* **B 650** (2003) 391 [hep-ph/0206071].

[18] H.-C. Cheng, J.L. Feng and K.T. Matchev, *Kaluza-Klein dark matter*, *Phys. Rev. Lett.* **89** (2002) 211301 [hep-ph/0207125].

[19] M. Battaglia, A. Datta, A. De Roeck, K. Kong and K.T. Matchev, *Contrasting supersymmetry and universal extra dimensions at the CLIC multi-TeV e^+e^- collider*, *JHEP* **07** (2005) 033 [hep-ph/0502041].

[20] S.Y. Choi, K. Hagiwara, H.U. Martyn, K. Mawatari and P.M. Zerwas, *Spin analysis of supersymmetric particles*, *Eur. Phys. J.* **C 51** (2007) 753 [hep-ph/0612301].

[21] A. Pukhov, *CalcHEP* 3.2*: MSSM, structure functions, event generation, batchs and generation of matrix elements for other packages*, hep-ph/0412191.

[22] A. Pukhov et al., *CompHEP: a package for evaluation of Feynman diagrams and integration over multi-particle phase space. User's manual for version* 33, hep-ph/9908288.

[23] CompHEP collaboration, E. Boos et al., *CompHEP* 4.4*: automatic computations from lagrangians to events*, *Nucl. Instrum. Meth.* **A534** (2004) 250 [hep-ph/0403113].

[24] Our CalcHEP files are available at http//theory.fnal.gov/people/kckong/6D.

[25] D.S. Gorbunov and A.V. Semenov, *CompHEP package with light gravitino and sgoldstinos*, hep-ph/0111291.

[26] G.A. Moortgat-Pick et al., *The role of polarized positrons and electrons in revealing fundamental interactions at the linear collider*, hep-ph/0507011.

[27] H.-C. Cheng, K.T. Matchev and M. Schmaltz, *Bosonic supersymmetry? Getting fooled at the LHC*, *Phys. Rev.* **D 66** (2002) 056006 [hep-ph/0205314].

[28] V.D. Barger, K.-m. Cheung, A. Djouadi, B.A. Kniehl and P.M. Zerwas, *Higgs bosons: intermediate mass range at e^+e^- colliders*, *Phys. Rev.* **D 49** (1994) 79 [hep-ph/9306270].

[29] A. Freitas, *Weakly coupled neutral gauge bosons at future linear colliders*, *Phys. Rev.* **D 70** (2004) 015008 [hep-ph/0403288].

JHEP02(2008)068